



Article

Unraveling the Arctic Sea Ice Change since the Middle of the Twentieth Century

Nathan Kong 1 and Wei Liu 2,*

- Bourns College of Engineering, University Honors Program, University of California Riverside, Riverside, CA 92521, USA
- Department of Earth and Planetary Sciences, University of California Riverside, Riverside, CA 92521, USA
- * Correspondence: wei.liu@ucr.edu

Abstract: Changes in Arctic sea ice since the middle of the last century are explored in this study. Both observations and climate model simulations show an overall sea ice expansion during 1953–1970 but a general sea ice decline afterward. Anthropogenic aerosols, nature forcing and atmospheric ozone changes are found to contribute to the sea ice expansion in the early period. Their effects are strong generally in late boreal summer. On the other hand, greenhouse gas warming has a dominant effect on diminishing Arctic sea ice cover during 1971–2005, especially in September. Internal climate variability also plays a role in the Arctic sea ice change during 1953–1970. However, it cannot solely explain the Arctic sea ice decline since the 1970s.

Keywords: Arctic sea ice; external forcing; internal climate variability

1. Introduction

Satellite coverage starting from 1979, has shown clear evidence of a substantial decrease in the Arctic sea ice cover [1–6]. However, prior to 1979, many observations and reconstructions have shown an increase in sea ice extent between the 1950s and 1970s [7–13]. These observed Arctic sea ice changes have been well simulated in historical experiments forced by a combination of anthropogenic and natural agents with climate models from Coupled Model Intercomparison Project (CMIP) phase 3 (CMIP3) [14] and phase 5 (CMIP5) [12,13]. Given the significant global and regional climate impacts of Arctic sea ice change [15–22], it is of central importance to understand the underlying physical mechanisms controlling the Arctic sea ice change during the past decades.

Changes in Arctic sea ice since the mid-twentieth century have been attributed to either external forcings [5,12–14,23] or internal climate variability [7,8,10]. For example, Gagne et al. [12] used the CMIP5 model CanESM2 historical simulations and associated anthropogenic aerosols forcing only, well-mixed greenhouse gases forcing only and natural forcing only experiments to show that the expansion of Arctic sea ice cover within 1950–1975 is mainly driven by anthropogenic aerosols. Mueller et al. [13] employed historical, well-mixed greenhouse gases and natural forcing only experiments with eight CMIP5 models and suggested that the negative sea ice trend induced by well-mixed greenhouse gases is partially offset by a weak positive trend induced by other anthropogenic forcings (mainly aerosols) over 1953–2012. On the other hand, Ployakov et al. [7] found a multidecadal oscillation that dominates the sea ice variability in the Kara, Laptev, East Siberian, and Chukchi Seas during the twentieth century.

The scientific question we are answering is if the historical Arctic sea ice increase and decline can be accurately simulated, and what the mechanism is for this. Unlike previous studies, we will leverage state-of-the-art CMIP phase 6 (CMIP6) models [24] and their historical and single forcing experiments [25] to probe the roles of external forcings and internal climate variability in driving the Arctic sea ice change since the mid-twentieth century. We will explore the role of atmospheric ozone change, which has been seldom discussed in previous studies.



Citation: Kong, N.; Liu, W.
Unraveling the Arctic Sea Ice Change since the Middle of the Twentieth
Century. Geosciences 2023, 13, 58.
https://doi.org/10.3390/
geosciences13020058

Academic Editors: Evgeny Chuvilin and Jesus Martinez-Frias

Received: 29 November 2022 Revised: 3 February 2023 Accepted: 12 February 2023 Published: 16 February 2023



Copyright: © 2023 by the authors. Licensee MDPI, Basel, Switzerland. This article is an open access article distributed under the terms and conditions of the Creative Commons Attribution (CC BY) license (https://creativecommons.org/licenses/by/4.0/).

Geosciences 2023, 13, 58 2 of 15

Furthermore, we will look into not only annual mean change but seasonal variation of Arctic sea ice as well, which also have not been widely discussed prior.

In our next section, we will address the materials we used in our analysis along with the methods employed on those materials. Subsequently, we will present our findings with a focus on the roles of external forcings and internal climate variability in historical Arctic sea ice changes. In our fourth and final section, we will conclude our study, along with further discussions.

2. Materials and Methods

2.1. Observations

We use two historical Arctic sea ice reconstructions: one is the Walsh and Chapman data set [26] (Walsh and Chapman thereafter) and the other is from HadISST [27]. The Walsh and Chapman data are a hybrid of satellite data with gridded data including those from the Scanning Multichannel Microwave Radiometer/Special Sensor Microwave/Imager, which provide one-degree gridded monthly sea ice extent and concentration starting from 1850. The HadISST data are created in the Met Office Hadley Centre, which contain the Hadley Centre sea ice and sea surface temperature. The HadISST observations consist of monthly sea ice concentration on a one-degree grid starting from 1870. We calculate the sea ice extent as the integral sum of the areas of all grid cells with a sea ice concentration of at least 15%. Both Walsh and Chapman and HadISST data are in-filled data. In the Walsh and Chapman data, a climatological infilling is used to close gaps in the historical record. In the HadISST data, Arctic sea ice concentrations present a data gap prior to 1953. As a result, we will focus on the Arctic sea ice changes in both observational datasets from 1953 onward.

2.2. Observations CMIP5 and CMIP6 Models and Simulations

We leverage 8 CMIP5 [28] and 13 CMIP6 [24] climate models to explore the mechanism of historical Arctic sea ice change (Table 1). We select these models in that they provide single-forcing simulations under historical changes in anthropogenic aerosols only (AER), well-mixed greenhouse gases only (GHG), natural sources such as solar and volcanic activity only (NAT) and atmospheric ozone only (OZONE), as well as the combined effect of all forcing (HIST). Because most of the CMIP5 and CMIP6 simulations end in 2005 and 2014, respectively, we focus on the period of 1953–2005, during which all the data are available from either observations or CMIP5 and CMIP6 model simulations.

We analyze the multi-model means (MMMs) of CMIP5/6 historical and single-forcing simulations to isolate and quantify the effects of individual external forcings on Arctic sea ice change. For either CMIP5 or CMIP6 models, we compute the MMM by first calculating the ensemble mean for each model and then averaging the mean values over all the models. Besides, we compute the inter-model spread using one standard deviation among the ensemble means of individual models.

Particularly, we analyze large (>30) ensemble simulations with three CMIP6 climate models, ACCESS1-ESM1.5, IPSL-CM6A-LR and MIROC6 (Table 1), to examine the effect of internal climate variability on Arctic sea ice change. Because the predictability horizon of climate models at most amounts to one to two decades [29,30], each individual ensemble member responds to anthropogenic forcing and meanwhile contains a realization of internal climate variability of a different timing from the others. Thereby, for each model, we calculate the ensemble mean to average out internal climate variability and obtain the model response to anthropogenic forcing. Then, we subtract the ensemble mean from each member to obtain the signals that represent internal climate variability.

It merits attention that: (i) The CMIP5 OZONE simulations cover changes in tropospheric and stratospheric ozone levels whereas the CMIP6 OZONE simulations are only forced by stratospheric ozone changes [25,31]. Unlike HIST, AER, GHG, and NAT simulations, only parts of the CMIP5 and CMIP6 models have OZONE simulations available (Table 1). (ii) Two CMIP5 models, CSIRO-Mk3.6.0 and NorESM1-M, are excluded from the

Geosciences 2023, 13, 58 3 of 15

analysis seeing that CSIRO-Mk3.6.0 has an unrealistic simulation of Arctic sea ice whereas NorESM1-M includes not only well-mixed greenhouse gases but also time-varying ozone changes in its GHG simulation [13]. (iii) The approach by Gagne et al. [12] is adopted in this study to directly estimate the aerosol effect on Arctic sea ice by means of AER simulations, which is different from that by Mueller et al. [13], in which the aerosol effect is indirectly estimated by subtracting the signals of GHG and NAT simulations from HIST simulations. (iv) The sum of sea ice changes in AER, GHG, NAT, and OZONE is not necessarily equal to the sea ice change in HIST due to other possible factors and/or the nonlinearity of responses to single forcings.

Table 1. The CMIP5 and CMIP6 models, simulations, and ensembles used in the current stu	Table 1.	. The CMIP5 and	CMIP6 models	, simulations	, and ensembles	used in the current s	tudv.
--	----------	-----------------	--------------	---------------	-----------------	-----------------------	-------

Models	HIST	AER	GHG	NAT	OZONE
CMIP5					
CanESM2	r[1–5]i1p1	r[1–5]i1p4	r[1–5]i1p1	r[1–5]i1p1	r[1–5]i1p1
CCSM4	r[1–6]i1p1	r[1, 4, 6]i1p10	r[1, 4, 6]i1p10	r[1, 2, 4, 6]i1p1	r[1, 4, 6]i1p14
FGOALS-g2	r[1–5]i1p1	r2i1p1	r1i1p1	r[1–3]i1p1	r1i1p1
GFDL-CM3	r[1–5]i1p1	r[1, 3, 5]i1p1	r[1, 3, 5]i1p1	r[1, 3, 5]i1p1	111171
GFDL-ESM2M	r1i1p1	r1i1p5	r1i1p1	r1i1p1	
GISS-E2-H	r[1–6]i1p1	r[1–5]i1p107	r[1–5]i1p1	r[1–5]i1p1	r[1-5]i1p105
GISS-E2-R	r[1–6]i1p1	r[1–5]i1p107	r[1–5]i1p1	r[1–5]i1p1	r[1–5]i1p105
IPSL-CM5A-LR	r[1–6]i1p1	r1i1p3	r[1-3]i1p1	r[1–3]i1p1	
CMIP6					
ACCESS-CM2	r[1-5]i1p1f1	r[1-3]i1p1f1	r[1-3]i1p1f1	r[1-3]i1p1f1	
ACCESS-ESM1.5	r[1-40]i1p1f1	r[1–3]i1p1f1	r[1–3]i1p1f1	r[1–3]i1p1f1	
BCC-CSM2-MR	r[1–3]i1p1f1	r[1-3]i1p1f1	r[1–3]i1p1f1	r[1–3]i1p1f1	
CanESM5	r[1–25]i1p1f1	r[1-10]i1p1f1	r[1–10]i1p1f1	r[1-25]i1p1f1	r[1-10]i1p1f1
CESM2	r[1–10]i1p1f1	r[1,3]i1p1f1	r1i1p1f1	r[1,3]i1p1f1	1
CNRM-CM6-1	r[1–20]i1p1f2	r[1-10]i1p1f2	r[1–10]i1p1f2	r[1-10]i1p1f2	
FGOALS-g3	r[1–6]i1p1f1	r[1-3]i1p1f1	r[1-3]i1p1f1	r[1-3]i1p1f1	
GFDL-ESM4	r[1-3]i1p1f1	r1i1p1f1	r1i1p1f1	r[1–3]i1p1f1	
HadGEM3-GC31-LL	r[1–5]i1p1f3	r[1–5]i1p1f3	r[1–5]i1p1f3	r[1-10]i1p1f3	
IPSL-CM6A-LR	r[1–33]i1p1f1	r[1–10]i1p1f1	r[1–10]i1p1f1	r[1-10]i1p1f1	r[1-10]i1p1f1
MIROC6	r[1–50]i1p1f1	r[1–10]i1p1f1	r[1-3]i1p1f1	r[1-50]i1p1f1	r[1-3]i1p1f1
MRI-ESM2.0	r[1–10]i1p1f1	r[1–5]i1p1f1	r[1–5]i1p1f1	r[1-5]i1p1f1	r[1, 3, 5]i1p1f1
NorESM2-LM	r[1-3]i1p1f1	r[1-3]i1p1f1	r[1-3]i1p1f1	r[1-3]i1p1f1	r[1-3]i1p1f1

3. Results

3.1. The Role of External Forcing in Annual Mean Arctic Sea Ice Changes

We examine annual mean Arctic sea ice extents from both observations and CMIP5/6 historical simulations. Both Walsh and Chapman and HadISST data indicate an Arctic sea ice expansion during 1953–1970 (Figure 1), with a linear trend of 0.10×10^6 km²/decade in the former and a trend of 0.19×10^6 km²/decade in the latter (Figure 2). They also suggest an Arctic sea ice decline during 1971–2005, with the linear trends of -0.41×10^6 km²/decade and -0.40×10^6 km²/decade, respectively. These observed sea ice expansions and declines have been generally well simulated by the CMIP5/6 models (Figures 1 and 2a,f). The MMMs of CMIP5 and CMIP6 historical simulations show Arctic sea ice increases in the trends of 0.17×10^6 km²/decade and 0.18×10^6 km²/decade over 1953–1970 but Arctic sea ice decreases in the trends of -0.19×10^6 km²/decade and -0.31×10^6 km²/decade over 1971–2005. It is also useful to note that climate models show large inter-model uncertainty in simulating the historical Arctic sea ice change, especially for CMIP5 models in the early period. The linear trend of Arctic sea ice extent may drop to a negative value for a particular CMIP5 model over 1953–1970 (Figure 3).

Geosciences **2023**, 13, 58 4 of 15

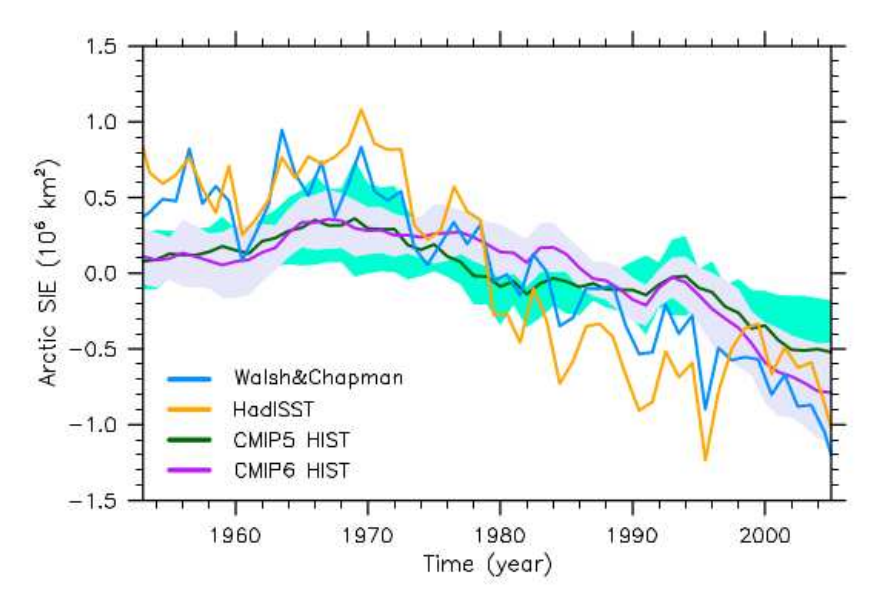


Figure 1. Annual mean Arctic sea ice extents (relative to the 1953–2005 average) from Walsh and Chapman (blue) and HadISST (orange) data and CMIP5 (MMM, green; inter-model spread, light green) and CMIP6 (MMM, purple; inter-model spread, light purple) historical simulations during 1953–2005. Sea ice extent is calculated as the integral sum of the areas of all grid cells with a sea ice concentration of at least 15%. The inter-model spread is calculated as one standard deviation among the ensemble means of individual models.

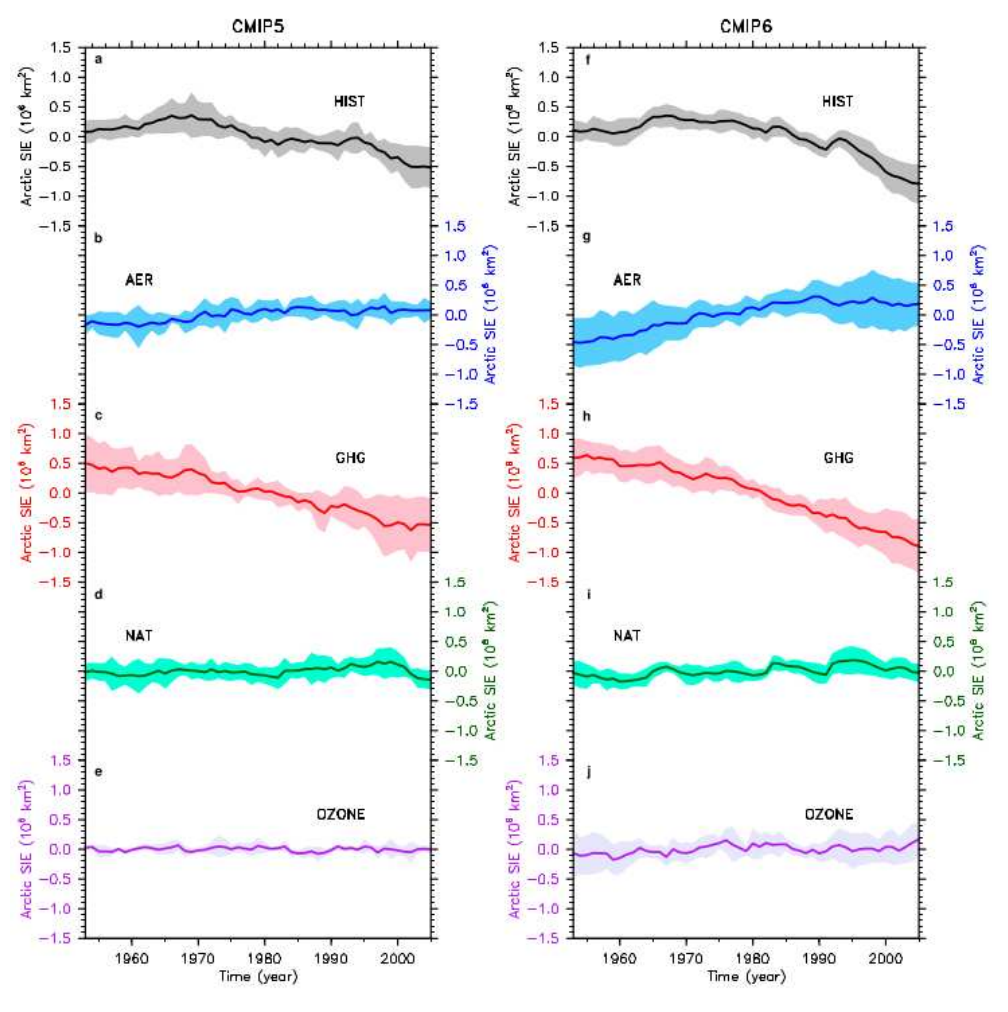


Figure 2. (a-e) Annual mean Arctic sea ice extents (relative to the 1953-2005 average) from CMIP5

Geosciences **2023**, *13*, *58* 5 of 15

historical (MMM, black; inter-model spread, gray), AER (MMM, blue; inter-model spread, light blue), GHG (MMM, red; inter-model spread, pink), NAT (MMM, green; inter-model spread, light green) and OZONE (MMM, purple; inter-model spread, light purple) simulations over 1953–2005. (f–j) Same as (a–e) but for CMIP6 simulations. Sea ice extent is calculated as the integral sum of the areas of all grid cells with a sea ice concentration of at least 15%. The inter-model spread is calculated as one standard deviation among the ensemble means of individual models.

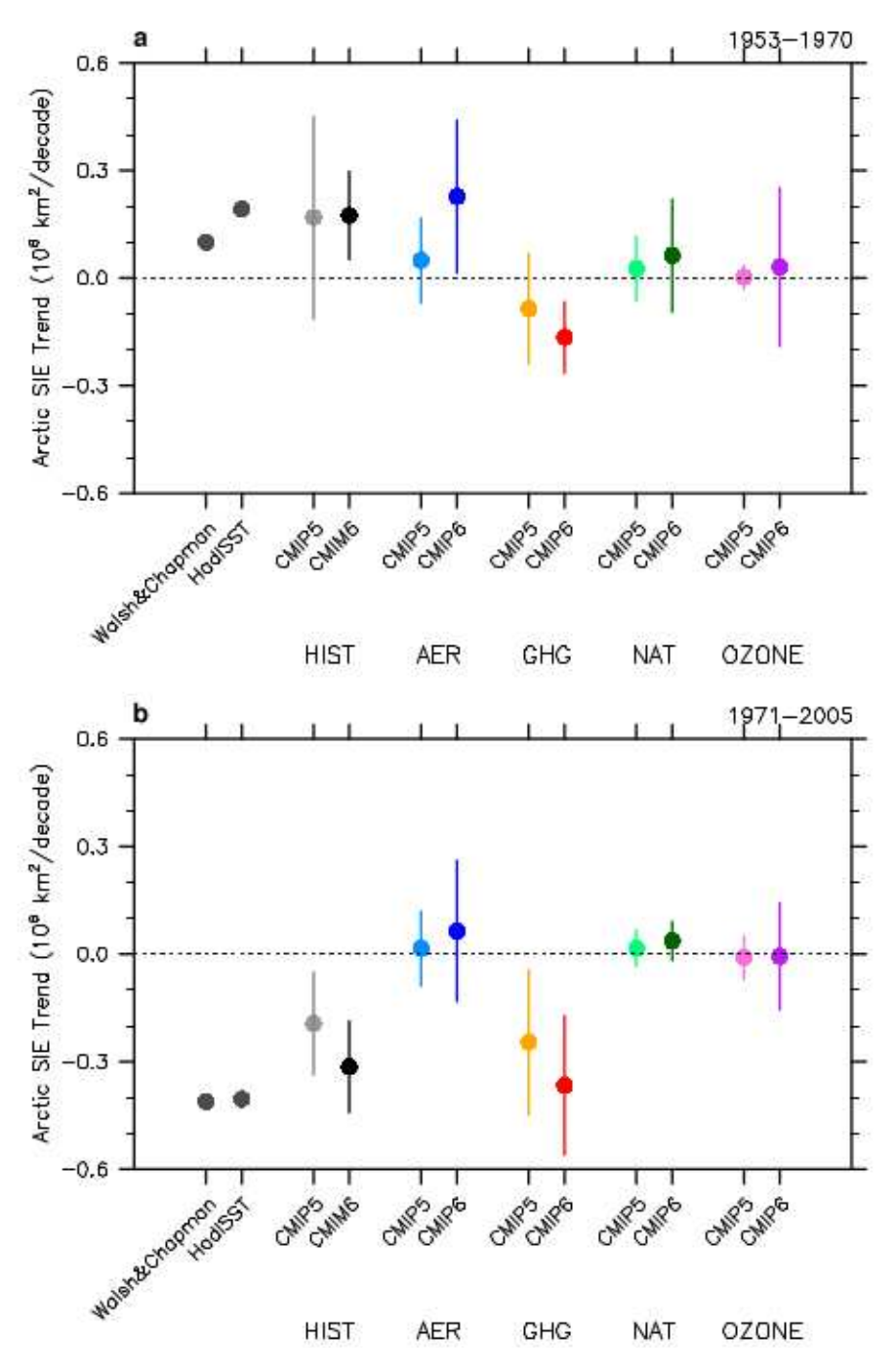


Figure 3. (a) Linear trends of annual mean Arctic sea ice extents from Walsh and Chapman and HadISST data (gray dots) and CMIP5 and CMIP6 historical (light gray and black), AER (light blue and blue), GHG (orange and red), NAT (light green and green) and OZONE (light purple and purple) simulations over 1953–1970. For the CMIP5/6 model's results, dots indicate MMMs, and bars indicate inter-model spreads. (b) Same as (a) but for trends over 1971–2005.

Geosciences **2023**, 13, 58 6 of 15

Though CMIP5/6 models capture the observed Arctic sea ice extent increase over 1953–1970, their patterns of sea ice concentration change are different from those of observations (Figure 4a–d). Particularly, the CMIP5/6 historical simulations show a general sea ice increase in the seas in and around the Arctic Ocean. Sea ice increases are especially robust in the Atlantic sector and in the Greenland and Barents Seas (Figure 4c,d). On the other hand, both observation datasets exhibit a strong sea ice increase in the Baffin Bay, the Greenland, Barents and Kara Seas but a strong sea ice decrease in the Chukchi and Bering Seas, and the Sea of Oshkosh (Figure 4a,b). These distinct regional sea ice changes are consistent with the previous results reported by Ployakov et al. [7] and Mahoney et al. [10].

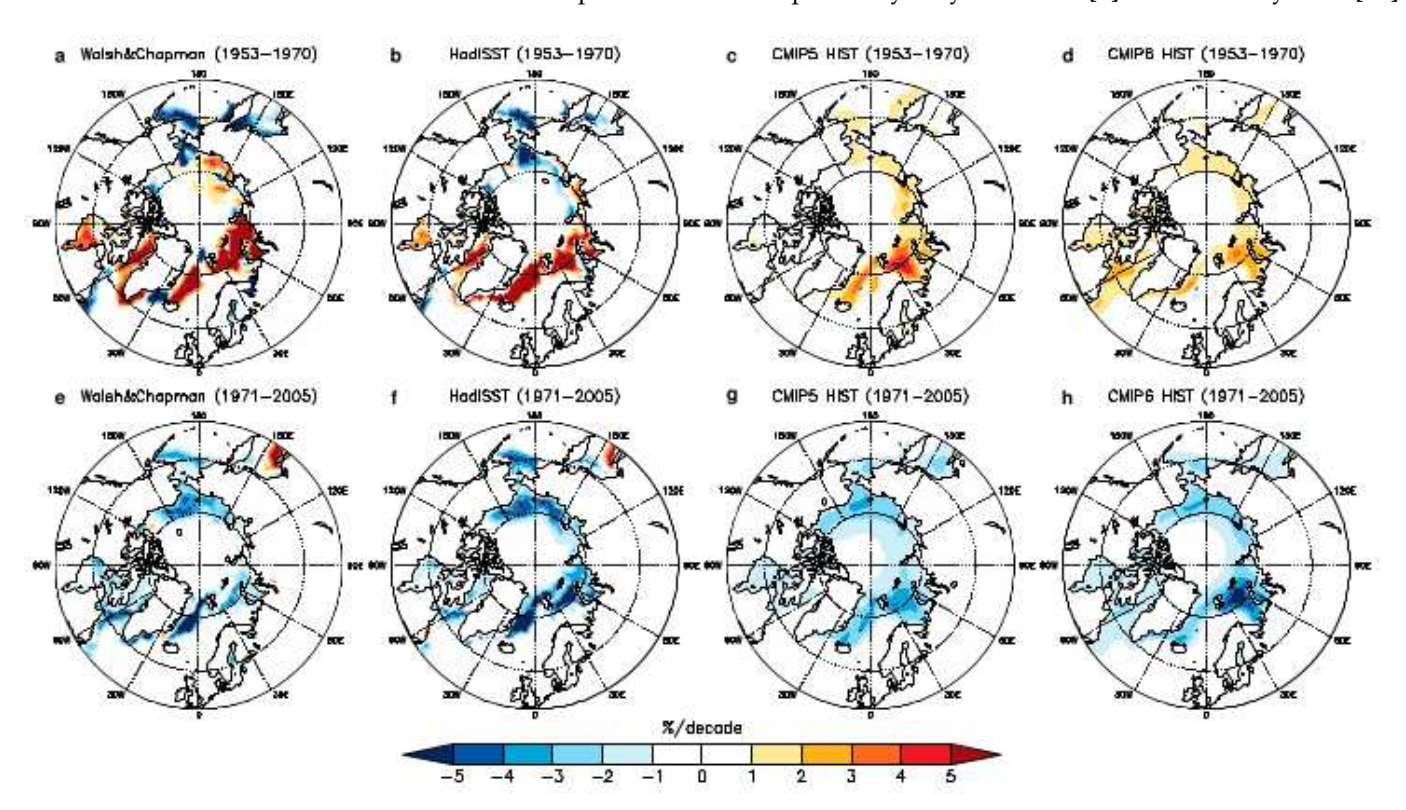


Figure 4. (a–d) Linear trends of annual mean sea ice concentrations (shading in percent/decade) from (a) Walsh and Chapman and (b) HadISST data and the MMMs of (c) CMIP5 and (d) CMIP6 historical simulations during 1953–1970. (e–h) Same as (a–d) but for the period of 1971–2005.

On the other hand, the CMIP5/6 models generally well simulate the observed pattern of sea ice concentration reduction during 1971–2005 (Figures 1 and 4). Both observations and CMIP5/6 historical simulations suggest a broad sea ice decrease in most seas in and around the Arctic Ocean (Figure 4e–h). The only exception occurs in the Sea of Oshkosh where observations indicate a sea ice increase while CMIP5/6 models simulate a sea ice decrease.

We further probe the role of external forcing in driving the annual mean sea ice change during different periods. Over 1953–1970, anthropogenic aerosols help enlarge Arctic sea ice extent (Figure 2b,g), with linear trends of $0.05 \times 10^6~\rm km^2/decade$ and $0.23 \times 10^6~\rm km^2/decade$ for the MMMs of CMIP5 and CMIP6 models (Figure 3a). Sea ice increases mainly occur in the Chukchi, Beaufort and Bering Seas in CMIP5 models (Figure 5a) but over most of the sea in the Arctic and especially strong in the Barents Sea in CMIP6 models (Figure 5f). Compared to anthropogenic aerosols, nature forcing and ozone changes cause much weaker sea ice increases (Figures 2, 3 and 5). Together, these sea ice increases are offset by greenhouse-gas-induced sea ice decreases (Figure 2). The declines of greenhouse-gas-induced Arctic sea ice extent are at a rate of $-0.09 \times 10^6~\rm km^2/decade$ and $0.16 \times 10^6~\rm km^2/decade$ for the MMMs of CMIP5 and CMIP6 models, respectively (Figure 3b). It is worth noting that the sea-ice response to aerosols forcing on average is

Geosciences **2023**, 13, 58 7 of 15

stronger in CMIP6 models than that in CMIP5 models (Figure 3a), which is potentially related to the stronger aerosol cooling [32] and higher climate sensitivity [33,34] in CMIP6 models. Another alternative explanation is that aerosols forcing drive a sea ice decrease in the Greenland Sea in CMIP5 models (Figure 5a), which partially offsets the sea ice increases in other regions and hence slows down the overall expansion of Arctic sea ice cover.

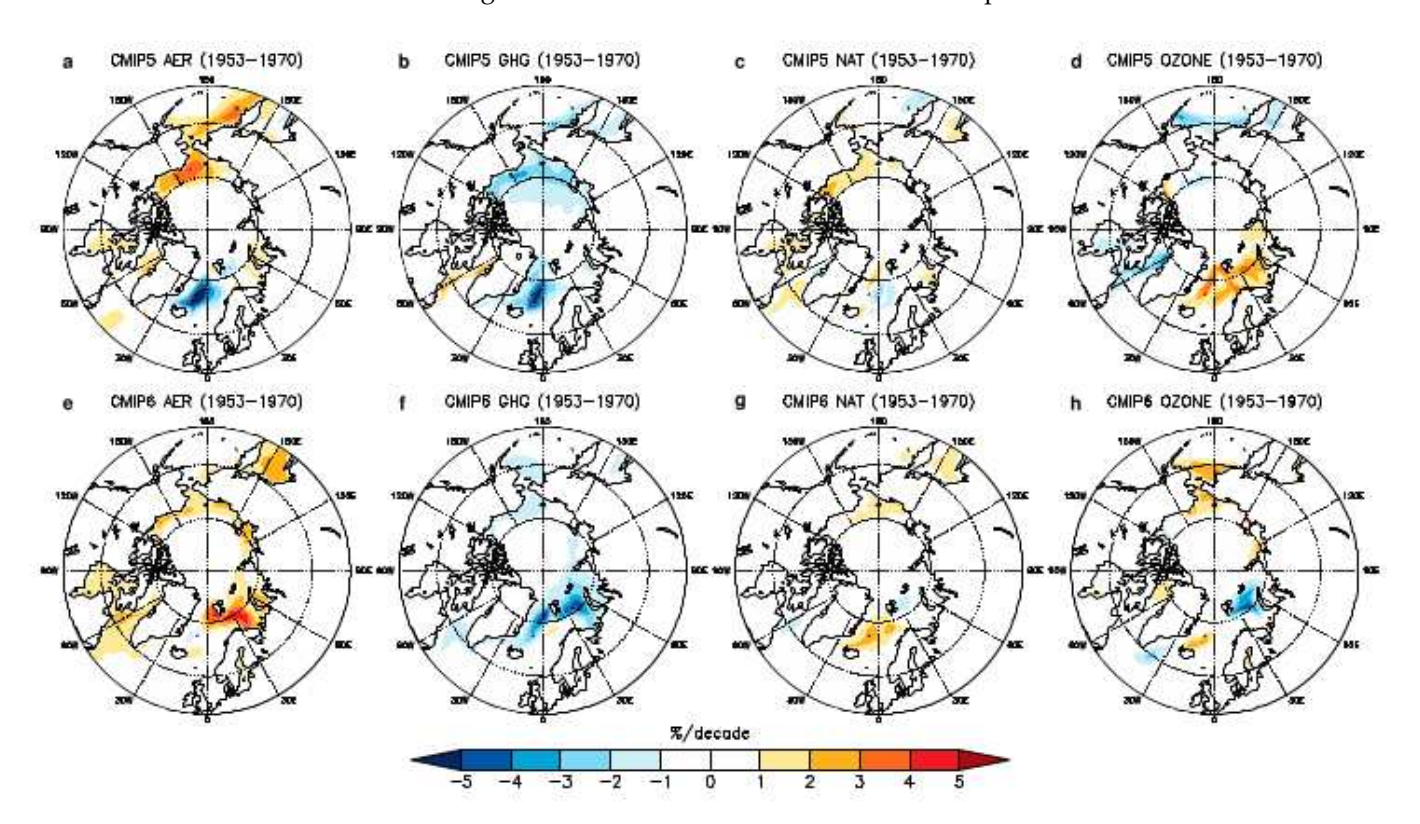


Figure 5. (a–d) Linear trends of annual mean sea ice concentrations (shading in percent/decade) for the MMMs of CMIP5 (a) AER, (b) GHG, (c) NAT, and (d) OZONE simulations during 1953–1970. (e–h) Same as (a–d) but for CMIP6 simulations.

Between 1971 and 2005, the effect of greenhouse gases becomes strong, leading to declining Arctic sea ice extents at rates of -0.25×10^6 km²/decade and 0.37×10^6 km²/decade for the MMMs of CMIP5 and CMIP6 models, respectively (Figure 3b). Though anthropogenic aerosols and natural forcings still act to enlarge Arctic sea ice extents (Figures 2 and 6), their effects are much smaller than that by greenhouse gases. The ozone effect on Arctic sea ice change is meanwhile neglectable. To summarize, greenhouse gas warming dominates the Arctic sea ice decline during 1971–2005.

3.2. The Role of External Forcing in Seasonal Arctic Sea Ice Variations

We compare the trends of monthly Arctic sea ice extent between observations and CMIP5/6 historical simulations over different time periods. During 1953–1970, both Walsh and Chapman and HadISST observations show a downward trend of Arctic sea ice extent in late spring (April–May) and an upward trend in July–December with the maximum trend in November (Figure 7a,c). By contrast, the MMMs of CMIP5/6 historical simulations illustrate upward trends of Arctic sea ice extent throughout seasons. The maximum trends occur in August and September in CMIP5 and CMIP6 models, respectively (Figure 7e,g). Over 1971–2005, both observations and CMIP5/6 historical simulations display downward trends of Arctic sea ice extent in all the months. The sea ice decline is especially strong in late boreal summer (Figure 7b,d,f,h).

Geosciences 2023, 13, 58 8 of 15

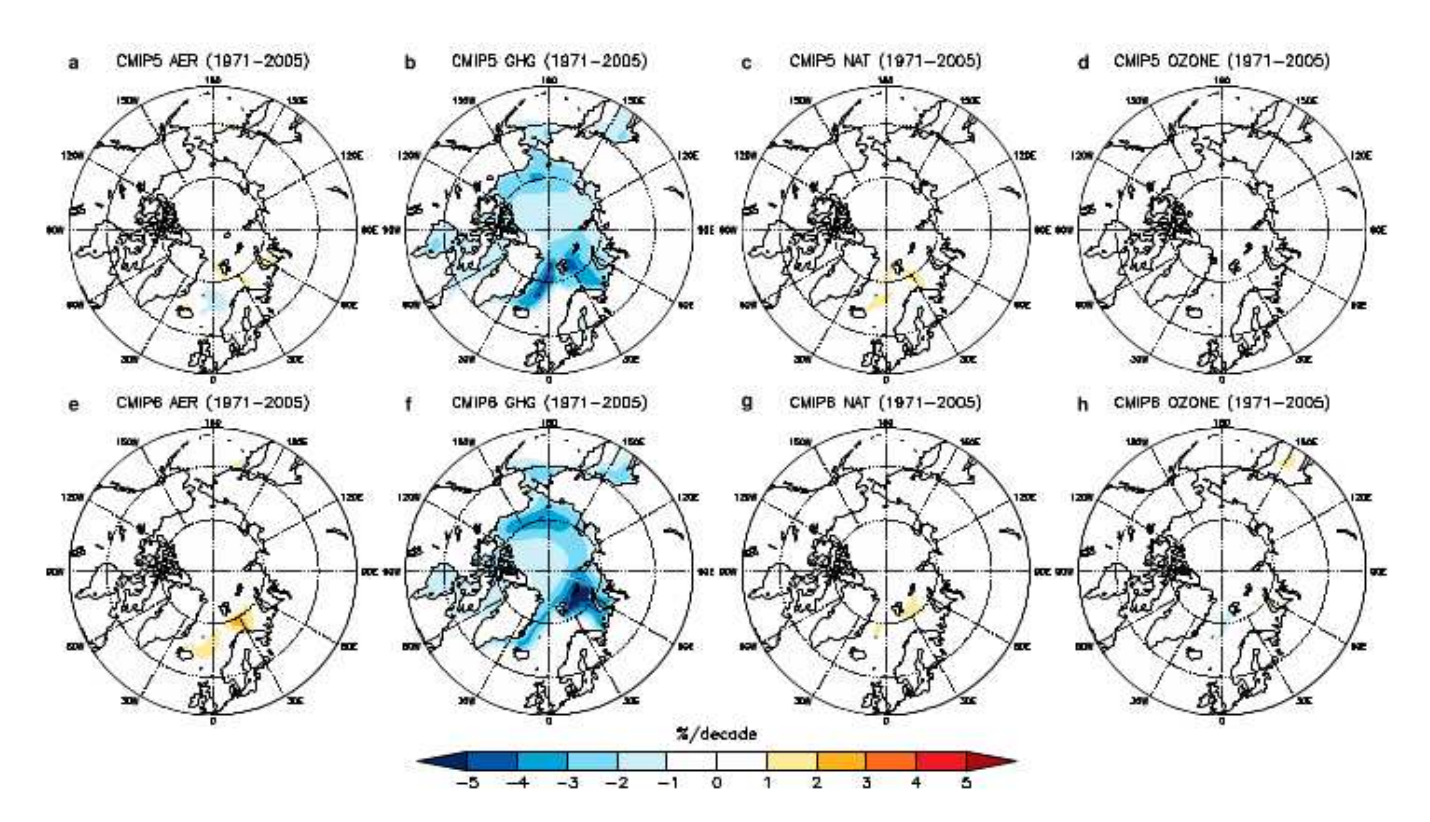


Figure 6. (**a**–**d**) Linear trends of annual mean sea ice concentrations (shading in percent/decade) for the MMMs of CMIP5 (**a**) AER, (**b**) GHG, (**c**) NAT, and (**d**) OZONE simulations during 1971–2005. (**e**–**h**) Same as (**a**–**d**) but for CMIP6 simulations.

We further probe the role of external forcing in driving seasonal sea ice variations during different periods. Over 1953–1970, both MMMs of CMIP5 and CMIP6 models show an aerosol-induced expansion and a greenhouse-gas-induced decline of Arctic sea ice extent across all the seasons (Figure 8). In September, we observe small sea ice increases for aerosols, natural forcings and ozone, and a decrease in sea ice for greenhouse gases. Between 1971 and 2005, both MMMs of CMIP5 and CMIP6 models show a dominant greenhouse-gas induced reduction in Arctic sea ice extent across seasons, which is most pronounced in September. Anthropogenic aerosols, natural forcings and atmospheric ozone changes drive small upward trends of Arctic sea ice extent in early boreal spring (Figure 9).

3.3. The Role of Internal Climate Variability in Historical Arctic Sea Ice Changes

To elucidate the role of internal climate variability in historical Arctic sea ice changes during the periods of 1953–1970 and 1971–2005, we remove the ensemble mean of Arctic sea ice extent trend from the trends of individual ensemble members for ACCESS-ESM1.5, IPSL-CM6A-LR and MIROC6, and compare these trends of individual members with those of Walsh and Chapman and HadISST observations for either period (Figure 10). Over 1953–1970, the observed trend of Arctic sea ice extent is within the inter-member spread in each of the three models, which indicates that internal climate variability can also play a role in Arctic sea ice change during this period [7,8,10]. Over 1971–2005, the observed trend of Arctic sea ice extent is outside the inter-member spread for any of the three models, suggesting that the reduction in Arctic sea ice extent during this period cannot be solely explained by internal climate variability. This result is consistent with previous studies [5,12–14,23] and highlights the importance of external forcings to the recent Arctic sea ice decline.

Geosciences 2023, 13, 58 9 of 15

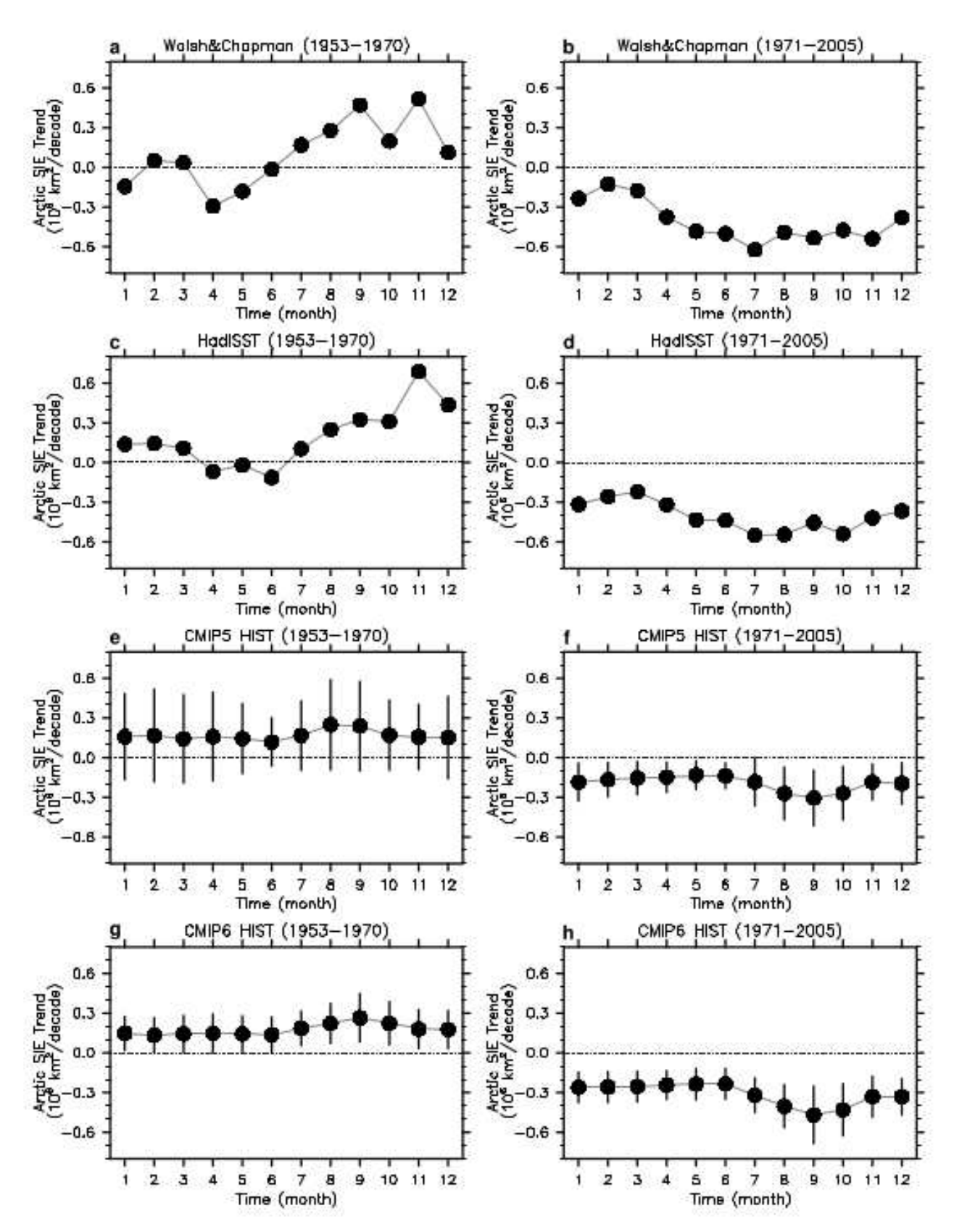


Figure 7. (a,c,e,g) Linear trends of monthly mean Arctic sea ice extents from (a) Walsh and Chapman and (c) HadISST data and (e) CMIP5 and (g) CMIP6 historical simulations over 1953–1970. For the CMIP5/6 model's results, dots indicate MMMs, and bars indicate inter-model spreads. (b,d,f,h) Same as (a,c,e,g) but for trends over 1971–2005.

Geosciences **2023**, 13, 58

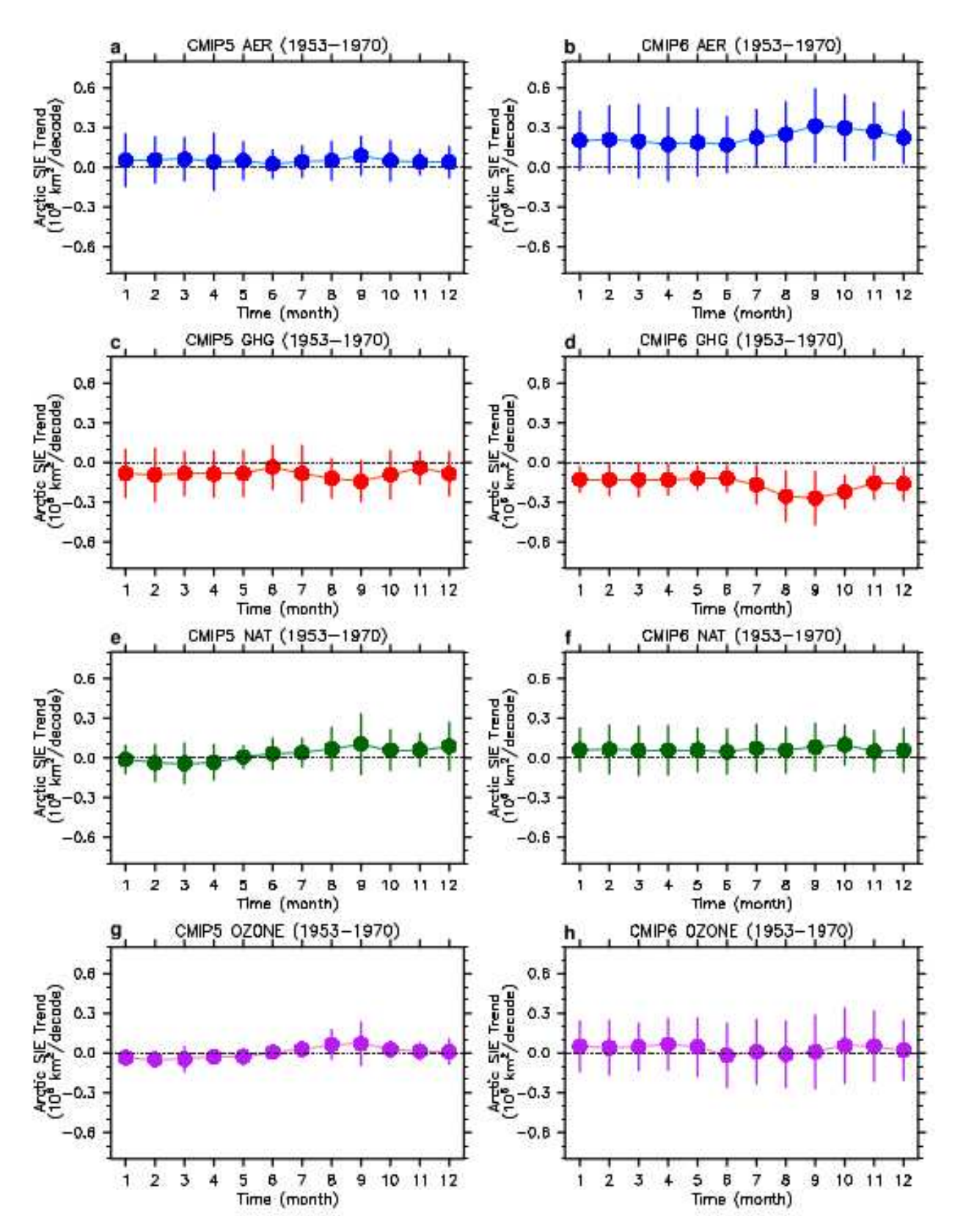


Figure 8. (a,c,e,g) Linear trends of monthly mean Arctic sea ice extents from CMIP5 (a) AER, (c) GHG, (e) NAT, and (g) OZONE simulations over 1953–1970. Dots indicate MMMs and bars indicate inter-model spreads. (b,d,f,h) Same as (a,c,e,g) but for CMIP6.

Geosciences 2023, 13, 58 11 of 15

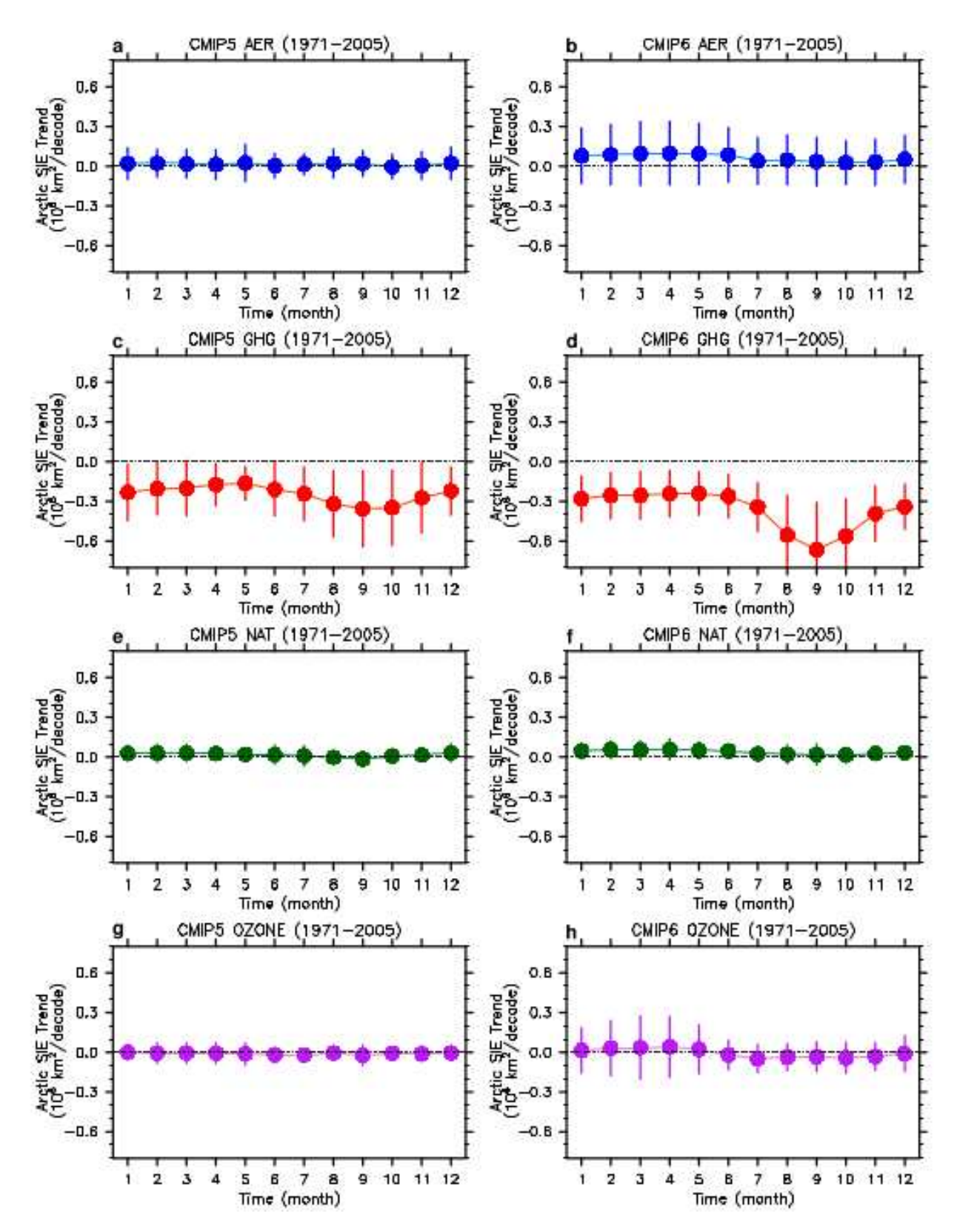


Figure 9. (a,c,e,g) Linear trends of monthly mean Arctic sea ice extents from CMIP5 (a) AER, (c) GHG, (e) NAT, and (g) OZONE simulations over 1971–2005. Dots indicate MMMs and bars indicate inter-model spreads. (b,d,f,h) Same as (a,c,e,g) but for CMIP6.

Geosciences 2023, 13, 58 12 of 15

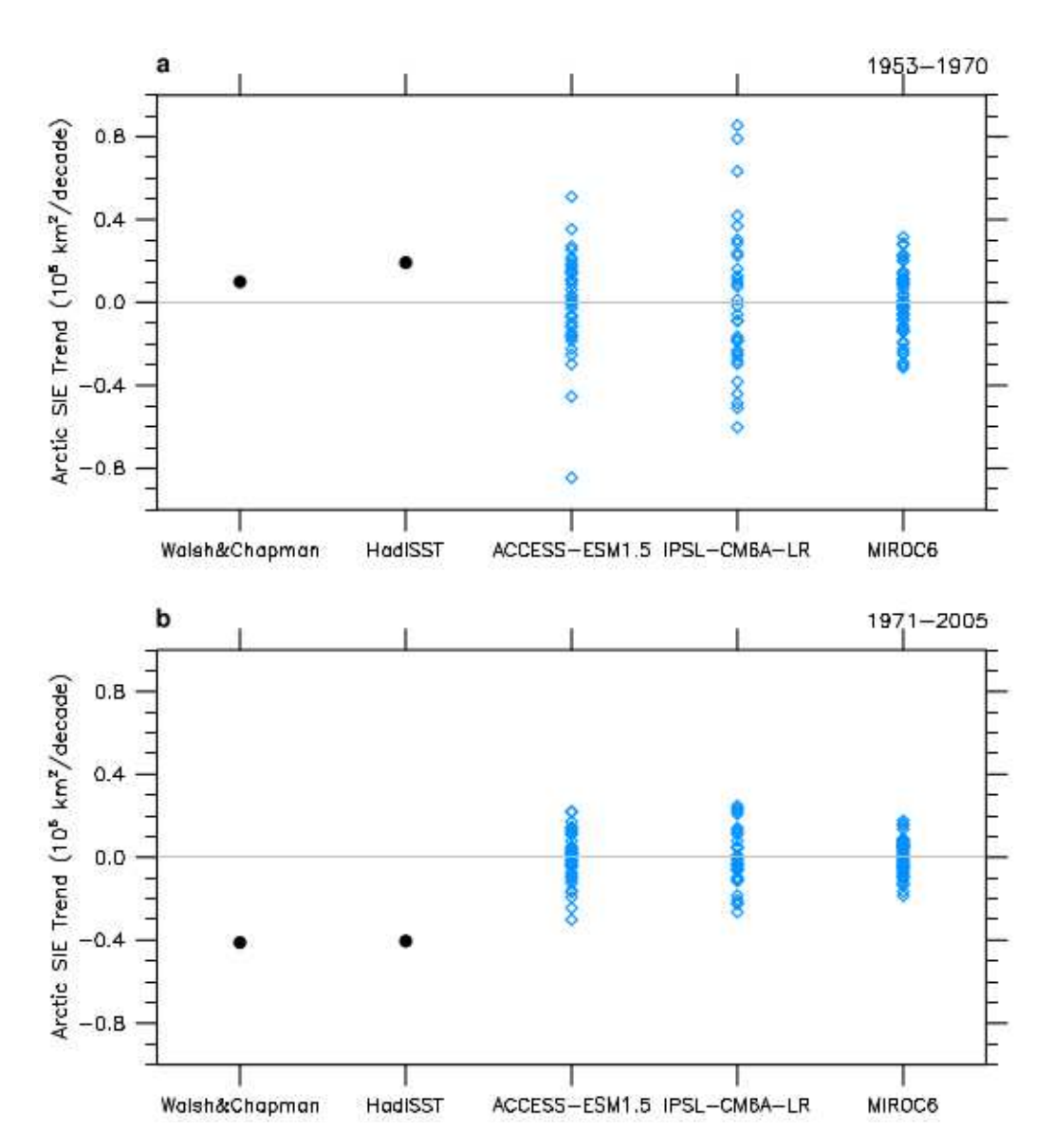


Figure 10. (a) Linear trends of annual mean Arctic sea ice extents from Walsh and Chapman and HadISST data (black) and ensemble members of ACCESS1-ESM1.5, IPSL-CM6A-LR and MIROC6 (blue) over 1953–1970. For each model, the ensemble mean of the trend is removed. (b) Same as (a) but for trends over 1971–2005.

4. Conclusions and Discussions

In this study, we explore the changes in Arctic sea ice since the middle of last century and associated physical mechanisms using Walsh and Chapman and HadISST observations and CMIP5 and CMIP6 climate models. Both observations and model simulations show consistent changes in sea ice extent—an increase over 1953–1970 and a decrease over 1971–2005—but distinct patterns of the change in sea ice concentration within the early period. Particularly, observations suggest a strong sea ice increase in the Baffin Bay, the Greenland, Barents and Kara Seas, but a strong sea ice decrease in the Chukchi and Bering Seas and the Sea of Oshkosh, whereas CMIP5/6 models simulate a general sea ice increase in the seas in and around the Arctic Ocean. Based on CMIP5/6 single forcing experiments, we further find that anthropogenic aerosols, nature forcing and ozone changes contribute to the sea ice expansion over 1953–1970, with marked effects generally during late boreal summer. From 1971 to 2005, the effect of greenhouse gas warming becomes dominant, which leads to a pronounced decline in Arctic sea ice over 1971–2005, especially in September. We also leverage large ensemble simulations of three CMIP6 models and discover that internal

Geosciences 2023, 13, 58 13 of 15

climate variability may play a role in the Arctic sea ice expansion over 1953–1970 but cannot fully explain the Arctic sea ice decline over 1971–2005.

Regarding the detailed physical processes, ocean circulation changes such as those in the Atlantic Meridional Overturning Circulation (AMOC) have been found to strongly influence the Arctic sea ice under either climate variability [7,35–37] or climate change [38]. The strength of the AMOC and its induced poleward heat transport significantly anticorrelate with Arctic sea ice extent [39–41]. Indeed, Liu and Fedorov [42] recently reported a two-way interaction between the changes in Arctic sea ice and the AMOC. Particularly, an Arctic sea ice decline can lead to a weakened AMOC with a multi-decadal delay by means of a downstream propagation of positive, sea-ice-induced buoyancy anomalies to the subpolar North Atlantic suppressing deep convection and deep-water formation there [20]. On the other hand, the weakened AMOC can promote an Arctic sea ice expansion within a few years by diminishing oceanic northward heat transport [43]. Further investigations are hence expected in future studies on the physical processes by which the atmosphere and oceans affect historical Arctic sea ice changes under individual external forcings and internal climate variability.

Author Contributions: Conceptualization, W.L.; methodology, N.K. and W.L.; validation, N.K. and W.L.; formal analysis, N.K.; investigation, N.K.; resources, W.L.; data curation, N.K.; writing—original draft preparation, N.K. and W.L.; writing—review and editing, N.K. and W.L.; visualization, N.K. and W.L.; supervision, W.L.; project administration, W.L.; funding acquisition, W.L. All authors have read and agreed to the published version of the manuscript.

Funding: This research was supported by Regents Faculty Development Award to W.L. W.L. was also supported by NSF (AGS 2053121, OCE 2123422 and AGS 2153486).

Institutional Review Board Statement: Not Applicable.

Informed Consent Statement: Not Applicable.

Data Availability Statement: The Walsh and Chapman data are available at ftp://sidads.colorado.edu/pub/DATASETS/NOAA/G10010/ [accessed on 21 June 2022]. The HadISST data are available at https://www.metoffice.gov.uk/hadobs/hadisst/data/download.html. [accessed on 21 June 2022]. The CMIP5 data are available at https://esgf-node.llnl.gov/search/cmip5/ [accessed on 21 June 2022]. The CMIP6 data are available at https://esgf-node.llnl.gov/projects/cmip6/ [Accessed on 21 June 2022].

Conflicts of Interest: The authors declare no conflict of interest.

References

- 1. Stroeve, J.; Holland, M.M.; Meier, W.; Scambos, T.; Serreze, M. Arctic sea ice decline: Faster than forecast. *Geophys. Res. Lett.* **2007**, 34, L09501. [CrossRef]
- 2. Serreze, M.C.; Holland, M.M.; Stroeve, J. Perspectives on the Arctic's shrinking sea-ice cover. *Science* **2007**, *315*, 1533–1536. [CrossRef]
- 3. Comiso, J.C.; Parkinson, C.L.; Gersten, R.; Stock, L. Accelerated decline in the Arctic sea ice cover. *Geophys. Res. Lett.* **2008**, 35, L01703. [CrossRef]
- 4. Parkinson, C.L.; Cavalieri, D.J. Arctic sea ice variability and trends, 1979–2006. J. Geophys. Res. Oceans 2008, 113, C07003. [CrossRef]
- 5. Notz, D.; Marotzke, J. Observations reveal external driver for Arctic sea-ice retreat. Geophys. Res. Lett. 2012, 39, L08502. [CrossRef]
- 6. Vihma, T. Effects of Arctic Sea Ice Decline on Weather and Climate: A Review. Surv. Geophys. 2014, 35, 1175–1214. [CrossRef]
- 7. Polyakov, I.V.; Alekseev, G.V.; Bekryaev, R.V.; Bhatt, U.S.; Colony, R.; Johnson, M.A.; Karklin, V.P.; Walsh, D.; Yulin, A.V. Long-term ice variability in Arctic marginal seas. *J. Clim.* **2003**, *16*, 2078–2085. [CrossRef]
- 8. Johannessen, O.M.; Bengtsson, L.; Miles, M.W.; Kuzmina, S.I.; Semenov, V.A.; Alekseev, G.V.; Nagurnyi, A.P.; Zakharov, V.F.; Bobylev, L.P.; Pettersson, L.H.; et al. Arctic climate change: Observed and modelled temperature and sea-ice variability. *Tellus* 2004, 56, 328–341. [CrossRef]
- 9. Meier, W.N.; Stroeve, J.; Fetterer, F. Whither Arctic sea ice? A clear signal of decline regionally, seasonally and extending beyond the satellite record. *Ann. Glaciol.* **2007**, *46*, 428–434. [CrossRef]
- 10. Mahoney, A.R.; Barry, R.G.; Smolyanitsky, V.; Fetterer, F. Observed sea ice extent in the Russian Arctic, 1933–2006. *J. Geophys. Res. Oceans* **2008**, *113*, C11005. [CrossRef]
- 11. Semenov, V.A.; Latif, M. The early twentieth century warming and winter Arctic sea ice. Cryosphere 2012, 6, 1231–1237. [CrossRef]

Geosciences **2023**, 13, 58 14 of 15

12. Gagné, M.-È.; Fyfe, J.C.; Gillett, N.P.; Polyakov, I.V.; Flato, G.M. Aerosol-driven increase in Arctic sea ice over the middle of the twentieth century. *Geophys. Res. Lett.* **2017**, *44*, 7338–7346. [CrossRef]

- 13. Mueller, B.L.; Gillett, N.P.; Monahan, A.H.; Zwiers, F.W. Attribution of Arctic Sea Ice Decline from 1953 to 2012 to Influences from Natural, Greenhouse Gas, and Anthropogenic Aerosol Forcing. *J. Clim.* **2018**, *31*, 7771–7787. [CrossRef]
- 14. Min, S.-K.; Zhang, X.; Zwiers, F.W.; Agnew, T. Human influence on Arctic sea ice detectable from early 1990s onwards. *Geophys. Res. Lett.* **2008**, *35*, L21701. [CrossRef]
- 15. Francis, J.A.; Chan, W.; Leathers, D.J.; Miller, J.R.; Veron, D.E. Winter Northern Hemisphere weather patterns remember summer Arctic sea-ice extent. *Geophys. Res. Lett.* **2009**, *36*, L07503. [CrossRef]
- 16. Overland, J.E.; Wang, M. Large-scale atmospheric circulation changes are associated with the recent loss of Arctic sea ice. *Tellus* **2010**, *62*, 1–9. [CrossRef]
- 17. Liu, J.; Curry, J.A.; Wang, H.; Song, M.; Horton, R.M. Impact of declining Arctic sea ice on winter snowfall. *Proc. Natl. Acad. Sci. USA* **2012**, *109*, 4074–4079. [CrossRef]
- 18. Cohen, J.; Screen, J.A.; Furtado, J.C.; Barlow, M.; Whittleston, D.; Coumou, D.; Francis, J.; Dethloff, K.; Entekhabi, D.; Overland, J.; et al. Recent Arctic amplification and extreme mid-latitude weather. *Nat. Geosci.* **2014**, *7*, 627–637. [CrossRef]
- 19. Deser, C.; Tomas, R.A.; Sun, L. The Role of Ocean–Atmosphere Coupling in the Zonal-Mean Atmospheric Response to Arctic Sea Ice Loss. *J. Clim.* **2015**, *28*, 2168–2186. [CrossRef]
- Liu, W.; Fedorov, A.; Sévellec, F. The Mechanisms of the Atlantic Meridional Overturning Circulation Slowdown Induced by Arctic Sea Ice Decline. J. Clim. 2019, 32, 977–996. [CrossRef]
- 21. Liu, W.; Fedorov, A.V. Global impacts of Arctic sea ice loss mediated by the Atlantic meridional overturning circulation. *Geophys. Res. Lett.* **2019**, *46*, 944–952. [CrossRef]
- 22. Taylor, P.C.; Boeke, R.C.; Boisvert, L.N.; Feldl, N.; Henry, M.; Huang, Y.; Langen, P.L.; Liu, W.; Pithan, F.; Sejas, S.A.; et al. Process Drivers, Inter-Model Spread, and the Path Forward: A Review of Amplified Arctic Warming. *Front. Earth Sci.* **2022**, *9*, 758361. [CrossRef]
- 23. Gregory, J.M.; Stott, P.A.; Cresswell, D.J.; Rayner, N.A.; Gordon, C.; Sexton, D.M.H. Recent and future changes in Arctic sea ice simulated by the HadCM3 AOGCM. *Geophys. Res. Lett.* **2002**, *29*, 2175. [CrossRef]
- 24. Eyring, V.; Bony, S.; Meehl, G.A.; Senior, C.A.; Stevens, B.; Stouffer, R.J.; Taylor, K.E. Overview of the Coupled Model Intercomparison Project Phase 6 (CMIP6) experimental design and organization. *Geosci. Model Dev.* **2016**, *9*, 1937–1958. [CrossRef]
- Gillett, N.P.; Shiogama, H.; Funke, B.; Hegerl, G.; Knutti, R.; Matthes, K.; Santer, B.D.; Stone, D.; Tebaldi, C. The Detection and Attribution Model Intercomparison Project (DAMIP v1.0) contribution to CMIP6. Geosci. Model Dev. 2016, 9, 3685–3697.
 [CrossRef]
- 26. Walsh, J.E.; Chapman, W.L. 20th-century sea-ice variations from observational data. Ann. Glaciol. 2001, 33, 444–448. [CrossRef]
- 27. Rayner, N.A.; Parker, D.E.; Horton, E.B.; Folland, C.K.; Alexander, L.V.; Rowell, D.P.; Kent, E.C.; Kaplan, A. Global analyses of sea surface temperature, sea ice, and night marine air temperature since the late nineteenth century. *J. Geophys. Res. Atmos.* 2003, 108, 4407. [CrossRef]
- 28. Taylor, K.E.; Stouffer, R.J.; Meehl, G.A. An Overview of CMIP5 and the Experiment Design. *Bull. Am. Meteorol. Soc.* **2012**, *93*, 485–498. [CrossRef]
- 29. Meehl, G.A.; Hu, A.; Tebaldi, C. Decadal prediction in the Pacific region. J. Clim. 2010, 23, 2959–2973. [CrossRef]
- 30. Ding, R.; Li, J.; Zheng, F.; Feng, J.; Liu, D. Estimating the limit of decadal-scale climate predictability using observational data. *Clim. Dyn.* **2016**, *46*, 1563–1580. [CrossRef]
- 31. Liu, W.; Hegglin, M.I.; Checa-Garcia, R.; Li, S.; Gillett, N.P.; Lyu, K.; Zhang, X.; Swart, N.C. Stratospheric ozone depletion and tropospheric ozone increases drive Southern Ocean interior warming. *Nat. Clim. Chang.* **2022**, *12*, 365–372. [CrossRef]
- 32. Dittus, A.J.; Hawkins, E.; Wilcox, L.J.; Sutton, R.T.; Smith, C.J.; Andrews, M.B.; Forster, P.M. Sensitivity of historical climate simulations to uncertain aerosol forcing. *Geophys. Res. Lett.* **2020**, *47*, e2019GL085806. [CrossRef]
- 33. Meehl, G.A.; Senior, C.A.; Eyring, V.; Flato, G.; Lamarque, J.F.; Stouffer, R.J.; Taylor, K.E.; Schlund, M. Context for interpreting equilibrium climate sensitivity and transient climate response from the CMIP6 Earth system models. *Sci. Adv.* **2020**, *6*, eaba1981. [CrossRef]
- 34. Zelinka, M.D.; Myers, T.A.; McCoy, D.T.; Po-Chedley, S.; Caldwell, P.M.; Ceppi, P.; Klein, S.A.; Taylor, K.E. Causes of higher climate sensitivity in CMIP6 models. *Geophys. Res. Lett.* **2020**, *47*, e2019GL085782. [CrossRef]
- 35. Frankcombe, L.M.; von der Heydt, A.; Dijkstra, H.A. North Atlantic multidecadal climate variability: An investigation of dominant time scales and processes. *J. Clim.* **2010**, *23*, 3626–3638. [CrossRef]
- 36. Drinkwater, K.F.; Miles, M.; Medhaug, I.; Otterå, O.H.; Kristiansen, T.; Sundby, S.; Gao, Y. The Atlantic Multidecadal Oscillation: Its manifestations and impacts with special emphasis on the Atlantic region north of 60°N. *J. Mar. Syst.* **2014**, *133*, 117–130. [CrossRef]
- 37. Delworth, T.L.; Zeng, F.; Vecchi, G.A.; Yang, X.; Zhang, L.; Zhang, R. The North Atlantic Oscillation as a driver of rapid climate change in the Northern Hemisphere. *Nat. Geosci.* **2016**, *9*, 509–512. [CrossRef]
- 38. Liu, W.; Fedorov, A.V.; Xie, S.-P.; Hu, S. Climate impacts of a weakened Atlantic Meridional Overturning Circulation in a warming climate. *Sci. Adv.* **2020**, *6*, eaaz4876. [CrossRef]
- 39. Mahajan, S.; Zhang, R.; Delworth, T.L. Impact of the Atlantic Meridional Overturning Circulation (AMOC) on Arctic surface air temperature and sea-ice variability. *J. Clim.* **2011**, *24*, 6573–6581. [CrossRef]

Geosciences **2023**, *13*, *58* 15 of 15

40. Day, J.J.; Hargreaves, J.C.; Annan, J.D.; Abe-Ouchi, A. Sources of multi-decadal variability in Arctic sea ice extent. *Environ. Res. Lett.* **2012**, *7*, 034011. [CrossRef]

- 41. Zhang, R. Mechanisms for low-frequency variability of summer Arctic sea ice extent. *Proc. Natl. Acad. Sci. USA* **2015**, 112, 4570–4575. [CrossRef] [PubMed]
- 42. Liu, W.; Fedorov, A. Interaction between Arctic sea ice and the Atlantic meridional overturning circulation in a warming climate. *Clim. Dyn.* **2022**, *58*, 1811–1827. [CrossRef]
- 43. Yeager, S.; Karspeck, A.; Danabasoglu, G. Predicted slowdown in the rate of Atlantic sea ice loss. *Geophys. Res. Lett.* **2015**, 42, 10704–10713. [CrossRef]

Disclaimer/Publisher's Note: The statements, opinions and data contained in all publications are solely those of the individual author(s) and contributor(s) and not of MDPI and/or the editor(s). MDPI and/or the editor(s) disclaim responsibility for any injury to people or property resulting from any ideas, methods, instructions or products referred to in the content.